Super-resolution in 4D positron emission tomography

D. Wallach, *Student Member, IEEE,* F. Lamare, J. Rubio, M. J. Ledesma-Carbayo, G. Kontaxakis, *Senior Member, IEEE*, A. Santos, *Senior Member, IEEE*, P. Maréchal, C. Roux, *Fellow IEEE,*, and D. Visvikis, *Senior Member, IEEE*

***Abstract*—Respiratory synchronized acquisitions lead to noisy images. Super-resolution techniques deal with the enhancement of several slightly different low-resolution images into a single high-resolution image. A maximum a-posteriori (MAP) super-resolution algorithm has been implemented and applied to respiratory gated PET images for motion compensation. The algorithm was tested on a GATE simulated datasets. It consisted of 8 frames of the NCAT phantom with lesions between 15-22mm placed throughout the lungs. Images were reconstructed using the OPLEM algorithm. Super-resolution was performed on the gated frames through a MAP algorithm, using a Huber prior as a regularization term to ensure convergence. The optimization of the function yielded by the MAP method was performed through a steepest descent algorithm. Motion fields were recovered using a previously presented elastic registration algorithm. Image enhancement was assessed by estimating signal to noise ratio (SNR) and contrast in regions of interest.**

I. Introduction

RESPIRATORY motion is a major source of reduced quality in Positron Emission Tomography (PET). In order to minimize its effects, it has been suggested to use respiratory synchronized acquisitions, which lead to gated frames [1]. Such frames, however, are of low signal-to-noise ratio (SNR) as they contain reduced statistics.

Several existing compensation techniques start with registering all the gated frames against a reference frame. All the warped images, now corresponding to the same part of the respiratory cycle, are subsequently summed. Arguing that the application of a linear process such as summation to iteratively (i.e. non-linearily) reconstructed frames is bound to lead to errors, some studies suggested the incorporation of deformations in into the reconstruction process.

All these techniques correct the effects of respiratory motion. Super-resolution techniques make use of the motion in a sequence of images in order to improve its quality. They aim at enhancing a low-resolution image belonging to a sequence of low-resolution images representing different looks of the same scene [2]. In the present study, a super-resolution algorithm is applied to the respiratory-gated PET images in order to improve the overall image quality of individual respiratory gated frames using the motion information present in all of the respiratory gated frames.

D. Wallach, C. Roux and D. Visvikis are with INSERM U650, LaTIM, Brest, France (e-mail: daphne.wallach@etudiant.univ-brest, Christian.Roux@telecom-bretagne.eu, dimitris@univ-brest.fr.) C. Roux is also with Telecom Bretagne, Brest, France

F. Lamare is with MRCCSC, Imperial College, London, United Kingdom (e-mail: frederic.lamare@csc.mrc.ac.uk.)

J. Rubio, M. J. Ledesma-Carbayo, G. Kontaxakis and A. Santos are with the ETSI Telecomunicación, Universidad Politécnica de Madrid, Madrid, Spain.

P. Maréchal is with Laboratoire MIP, Université Paul Sabatier, Toulouse, France.

II. Materials and Methods

A. Super-resolution algorithm

We use the maximum a posteriori (MAP) algorithm, which consists in inverting an observation model relating the low-resolution images (LR images) to the high-resolution image (HR image) (see Figure 1).

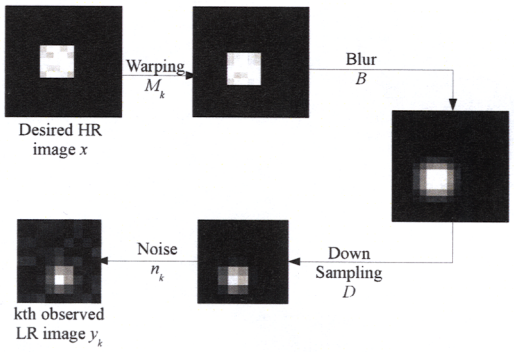

Fig. 1. Observation model

The observed LR images result from warping, blurring and subsampling of the HR image x. Moreover, each LR image is assumed to be corrupted by additive noise. The observation model can be written

$$y_k = DBM_k x + \varepsilon_k, \quad k = 1 \dots K, \tag{1}$$

where

- D is a subsampling matrix performing a mere averaging over neighbouring voxels,
- B is a blur matrix that models the action of the psf of the PET scanning machine,
- M_k is a warp matrix,
- ε_k is a lexicographically ordered noise vector representing modelling errors.

The warp matrices are obtained through the application of an elastic registration algorithm to the gated PET frames [3].

The operators D, B and M_k are known, and the LR images y_k are measured, the aim of super-resolution is the recovery of the HR image x. This is done by maximizing its *a posteriori* probability, that is to say the probability of x given the y_k. The function to maximize reads

$$F_1(x) = \mathbb{P}(x|y_1, y_2, \ldots, y_K) = \prod_{k=1}^{K} \mathbb{P}(x|y_k)$$

According to Bayes formula, this yields

$$\arg\max_x F_1(x) = \arg \max_x \prod_{k=1}^{K} \mathbb{P}(y_k|x)\mathbb{P}(x)$$

The noise ε_k is assumed to be gaussian, thus the conditionnal density $\mathbb{P}(y_k|x)$ is

$$\mathbb{P}(y_k|x) = \frac{1}{(\sqrt{2\pi\sigma_k^2})^N} \exp\left(-\frac{1}{2\sigma_k^2}||y_k - DBM_k x||^2\right)$$

where σ_k is the standard deviation of the kth LR image, and N is the dimension of the LR image.

The *a priori* image model $\mathbb{P}(x)$ is chosen as a Huber prior. It is of the form

$$\mathbb{P}(x) = \exp\left(-\lambda \sum_{j=1}^{N} \sum_{k \in \mathcal{N}_j} V(x_j - x_k)\right),$$

$\mathcal{N}_j$ being the neighbourhood of the voxel j. The Huber potential function is given by

$$V(x) = \begin{cases} \frac{z^2}{2\delta} & \text{if } |z| < \delta \\ |z| - \frac{\delta}{2} & \text{if } |z| \geq \delta. \end{cases}$$

It is quadratic near the origin and linear far from the origin: small intensity differences between neighbouring voxels are more penalized than large ones.

The function to minimize is the opposite of the log-likelihood:

$$F(x) = \frac{1}{2\sigma_k^2}||y_k - DBM_k x||^2 + \lambda \sum_{j=1}^{N} \sum_{k \in N_j} V(x_j - x_k)$$

The regularization parameters λ and δ are chosen through cross-validation [4]. F is minimized using a steepest descent algorithm.

B. Description of the datasets

The proposed algorithm was evaluated on a simulated PET image sequence.

It uses a digital NURBS base 4D cardiac torso phantom (NCAT). A set of eight NCAT emission images was produced throughout a respiratory cycle. Spherical lesions of 15 and 21 mm across were added to the NCAT emision and attenuation images.

GATE (Gate4 Application for Tomographic Emission) was used to perform an accurate simulation of the Philips Allegro PAT system. Used in combination with the NCAT phantom emission and attenuation images, it produced dynamic emission data sets acquired through a respiratory cycle. Finally, the list-mode data output of the simulation was used.

A total number of 5.4 million detected coincidences were simulated for each of the eight NCAT temporal frames. In addition, a total of 43.2 million coincidences (corresponding to the total coincidences simulated throughout a respiratory average acquisition) were simulated for the first NCAT emission frame.

Eventually, all images were reconstructed with the one-pass list mode EM (OPL-EM) algorithm.

C. Image analysis

The following images were compared :

- the first frame of the gated sequence, reconstructed in $128 \times 128 \times 60$ (*Upsampled Frame 1* image),
- the first frame of the sequence, reconstructed with the count statistics corresponding to the entire respiratory cycle in $128 \times 128 \times 60$ (*All Counts* image),
- the motion average image, reconstructed in $128 \times 128 \times 60$ with the list mode files corresponding to all the gated frames (*Motion Average* image),
- the sum of all gated frames reconstructed in $128 \times 128 \times 60$ and registered to frame 1 (*Sum of Registered Frames* image),
- the output of the proposed algorithm (*SR* image).

All images were put to a commmon resolution ($256 \times 256 \times 120$ voxels). The smaller images underwent a trilinear interpolation.

The improvement obtained as a result of the implemented super-resolution method described was assessed by measuring the difference in lesion's contrast as well as the lesion's signal-to-noise ratio compared to the *All Counts* image, which is our reference image. The difference for the SNR is calculated as follows:

$$\%\ \text{SNR difference} = \frac{\text{SNR}_{evaluated} - \text{SNR}_{Allcounts}}{\text{SNR}_{Allcounts}} * 100$$

The difference of contrast is calculated in a similar manner.

III. Results and discussion

Fig. 3 allows a direct comparison of super-resolution and the method consisting in summing the registered frames. Both methodologies lead to better images than the non-corrected ones, in terms of SNR as well as contrast. Respiratory motion is indeed compensated.

Super-resolution demonstrates better results than simply warping and summing the frames. It outperforms the other correction method by approximately 7% in terms of SNR recovery in the lesions and by 5% in terms of constrast recovery.

The SNR in the background has a different meaning than that in the lesions. It does not depend on motion, but only on the quantity of information considered. That is why the *Motion Average* and the *Sum of Registered Frames* images have similar

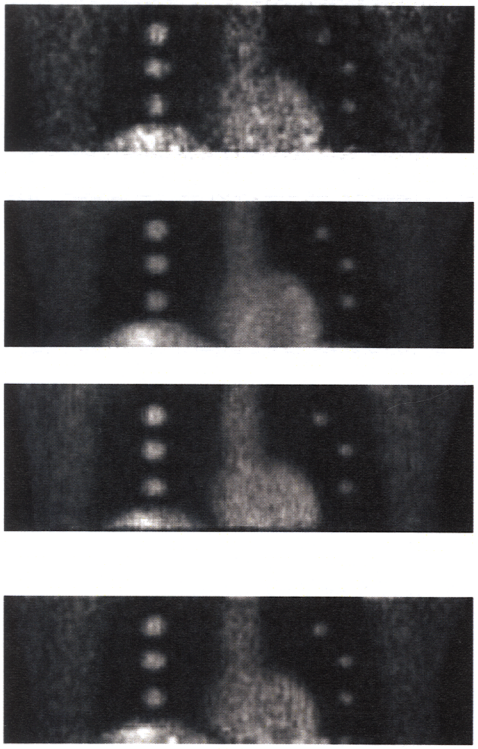

Fig. 2. Up to down: *Upsampled Frame 1* image, *All Counts* image, *Sum of Registered Frames* image and *SR* image

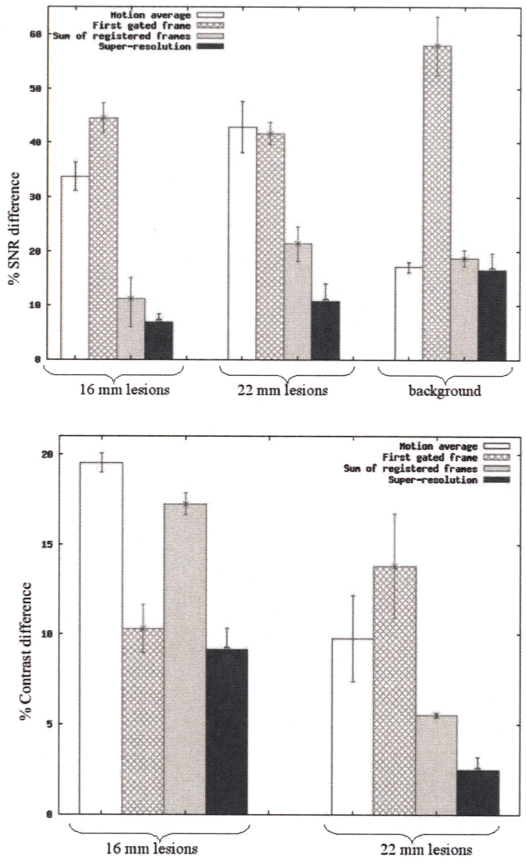

Fig. 3. Mean and standard deviation of the difference relative to the All counts image in signal-to-noise ratio and contrast, as a function of lesion size

results: they all contain all the information available. The *Upsampled Frame 1* image, containing only a fraction of the statistics, has a SNR very different from that of the *All Counts* image. The *SR* image uses all the frames in order to improve the quality of frame 1. The fact that this image performs as well as the *Motion Average* and the *Sum of Registered Frames* images in terms of SNR in the background shows that all the acquired information has indeed been used.

Both correcting methodologies perform better on larger lesions (particularly in terms of contrast). This is due to the registration being less accurate on smaller lesions. Hence, future work will consist in estimating the motion parameters during the super-resolution process. Motion parameters calculated on a high-resolution image are bound to be more accurate than the ones estimated on a noisy and blurred one.

Results could be further improved by incorporating the super-resolution process to the reconstruction. This will be also looked into in the future.

IV. Conclusion

A MAP based super-resolution algorithm has been implemented and applied to respiratory gated images. Results on a simulated dataset including realistic respiratory motion show that this method leads to motion compensation combined with improved image SNR and contrast. Future work will consist in estimating the motion parameters during the super-resolution process, and applying this method directly to raw data.

References

[1] L. Boucher, S. Rodrigue, R. Lecomte, and F. Benard, "Respiratory gating for 3-dimensional pet of the thorax: Feasibility and initial results," *J Nucl Med*, vol. 45, pp. 214–219, 2004.

[2] M. G. Kang and S. Chaudhuri, "Super-resolution image reconstruction," *Signal Processing Magazine, IEEE*, vol. 20, pp. 19–20, 2003.

[3] M. Ledesma-Carbayo, J. Kybic, M. Desco, A. Santos, M. Suhling, P. Hunziker, and M. Unser, "Spatio-temporal nonrigid registration for ultrasound cardiac motion estimation," *Medical Imaging, IEEE Transactions on*, vol. 24, pp. 1113–1126, 2005.

[4] L. C. Pickup, S. J. Roberts, and A. Zisserman, "Optimizing and learning for super-resolution," *Proceedings of the British Machine Vision Conference*, 2006.